SECOND EUROPEAN CONFERENCE ON EARTHQUAKE ENGINEERING
AND SEISMOLOGY, ISTANBUL AUG. 25-29, 2014

SEISMIC DAMAGE AND FAILURE ANALYSIS OF ARCH DAM WITH DIFFERENT MATERIAL MODELS OF FOUNDATION

Shengshan Guo[1], Deyu Li[2], Jin Tu[3], Houqun Chen[4]

ABSTRACT

In this study, a relatively complete nonlinear dynamic analysis model of arch dam-foundation-reservoir system based on finite element method in the time domain is presented. In this model, Lagrange multiplier method considering contraction joint opening and closing, nonlinear material models of concrete and rock considering dam and foundation, and viscous-spring boundary model considering radiation damping due to energy dissipation to the far field foundation are included. Since the analysis model and solving method coupling contact problem and nonlinear material model is very complex in the dam-foundation-reservoir system and enormous computation work is needed, massively parallel computation based on the domain decomposition method is introduced accordingly. Different material models considering foundation are used for comparison, including elastic model, damage model and Drucker-Prager elastoplastic model. The study of Shapai arch dam in China subjected to the Wenchuan earthquake is taken as an example. The result shows that different failure modes are got by using different material models of foundation, and the damage of dam-foundation system which has been simulated by using damage model for dam and foundation is close to the actual damage.
Keywords: arch dam; damage model; seismic response; contact force model; foundation radiation damping; parrallel computation

1 INTRODUCTION

Various models have been developed during the recent years for modeling the seismic damage response of arch dam. Cervera et al[1]. used an isotropic damage model which allows for tension and compression to analyze the seismic damage of an arch. Zhong et al[2]. studied seismic failure of concrete dams considering heterogeneity nature of the concrete material and the model was verified through a shaking table test. Pan et al[3]. used the extended finite element, plastic damage model, and Drucker－Prager elastoplastic model to compare the seismic damage of Dagangshan arch dam in China. Hariri-Ardebili et al[4]. used the coaxial rotating smeared crack approach to study the seismic response of KARADJ arch dam in Iran.

One of the most important aspects in the failure of non-homogeneous quasi-brittle material like concrete and rock is the initiation and propagation of microcracks. Macroscopic mechanical parameters are characterized by the evolution of the decreasing of strength and stiffness with the development of microcracks which eventually form into macroscopic crack. Therefore, damage model applied to the failure of concrete and rock is suitable and realistic.

In this paper, due to the complexity of dynamic property of rock mass, to explore the effect on the seismic damage response of arch dam using different material models for rock mass, some

[1] Doctor, China Institute of Water Resources and Hydropower Research, Beijing, guoss@iwhr.com
[2] Professor, China Institute of Water Resources and Hydropower Research, Beijing, lideyu@iwhr.com
[3] Professor, China Institute of Water Resources and Hydropower Research, Beijing, tujin@iwhr.com
[4] Professor, China Institute of Water Resources and Hydropower Research, Beijing, chenhq@iwhr.com

comparative investigations are taken. The seismic damage process of Shapai dam-foundation system is investigated by using damage model applied to dam-foundation system. As comparative studies, the seismic damage process of dam-foundation system is investigated by using damage model for dam, using Drucker-Prager elastoplastic and elastic model for rock mass. Since the computation is enormous, parallel computation is introduced in this paper and all computing work is completed by the parallel finite element program developed by China Institute of Water Resources and Hydropower Research.

2 Time domain dynamic equation

Dynamic equation after finite element discretization:

$$\mathbf{M}\ddot{\mathbf{U}} + \mathbf{C}\dot{\mathbf{U}} + \mathbf{K}\mathbf{U} = \mathbf{F} \tag{1}$$

Where, $\mathbf{M}$, $\mathbf{C}$ and $\mathbf{K}$ are the mass, damping and stiffness matrixes respectively, and $\mathbf{F}$, $\ddot{\mathbf{U}}$, $\dot{\mathbf{U}}$ and $\mathbf{U}$ are the load, acceleration, velocity and displacement vectors respectively. For large scale nonlinear dynamical calculations, the decoupled explicit integration algorithm is more efficient. Thus, this paper adopts the decoupled explicit numerical integration format which combines the center differential and unilateral differential method as:

$$\dot{\mathbf{U}}_{\mathrm{n}} = \frac{\mathbf{U}_{\mathrm{n}} - \mathbf{U}_{\mathrm{n-1}}}{dt}, \quad \ddot{\mathbf{U}}_{\mathrm{n}} = \frac{\mathbf{U}_{\mathrm{n+1}} - 2\mathbf{U}_{\mathrm{n}} + \mathbf{U}_{\mathrm{n-1}}}{dt^2}. \tag{2}$$

The discrete dynamic equation at time step n+1 is written as:

$$\mathbf{M}\mathbf{U}_{\mathrm{n+1}} = \mathbf{M}\left(2\mathbf{U}_{\mathrm{n}} - \mathbf{U}_{\mathrm{n-1}}\right) - \mathbf{K}\mathbf{U}_{\mathrm{n}}dt^2 - \mathbf{C}\left(\mathbf{U}_{\mathrm{n}} - \mathbf{U}_{\mathrm{n-1}}\right)dt + \mathbf{F}_{\mathrm{n}}dt^2 \tag{3}$$

If the diagonal lumped mass matrix $\mathbf{M}$ is used, the equation is solved explicitly.

3 Foundation radiation damping

For the seismic response of the dam, since foundation is infinite with respect to the dam, the seismic analysis of dam is actually to simulate the wave propagation of the open system consisting of infinite foundation and dam, which includes both the vibration of dam generated by the input wave and the scattering wave to the foundation generated by the dam as vibration source. The energy gradually escapes as the scattering wave transmits to the foundation due to the geometric spreading and damping dissipation. In the actual calculation, it is impossible to simulate the scattered wave dissipation process of infinite foundation, and the foundation can be only taken a limited range. Theoretically, as long as the scope of foundation meets the need of $L \geq CT/2$, where C is the velocity of foundation and T is the seismic wave duration, the dissipation effect can be included. In static analysis, the foundation far away from the dam could take a larger size grid, but in dynamic analysis oversized grid could not be taken due to the limit of the wave length. Thus, if the scope of foundation is taken by $L \geq CT/2$, considerable computing would be brought and difficulty to apply to engineering practice. If a smaller range of foundation is taken, the scattered wave which was supposed to spread to foundation would reflect back to dam and seismic response of dam would be amplified. The effect that energy spreads to foundation is equivalent to damping, so called 'foundation radiation damping'. In order to simulate the effect of 'foundation radiation damping', in the context of a limited range of foundation, the concept of artificial boundary is proposed to simulate the effect of infinite foundation to near –field wave.

Global artificial boundary and local artificial boundary are two main boundaries. Global artificial boundary[5,6] is based on the frequency domain and coupled equation is formed in space domain. To solve the coupled equation, cumbersome and enormous computation is needed. The nonlinearity of foundation can't be considered due to the frequency domain. Thus, the local artificial boundary which is a decoupled method in space and time domain is proposed. The local artificial boundary includes

displacement artificial boundary and stress artificial boundary. Transmitting boundary[7] belongs to displacement artificial boundary which has second –order accuracy, but the phenomenon of numerical instability may occur and usually requires repeatedly trial. Viscous-spring artificial boundary[8] belongs to stress artificial boundary, which needs to impose external force and spring-damping system on the boundary. The boundary nodes and internal nodes use a uniform format to solve and the algorithm has first order accuracy and good stability.

The viscous-spring artificial boundary is used in the present paper. This boundary condition is applied at the far –end boudanry of the foundation in 3D space given as :

$$\sigma = K_{\mathrm{n}}u + C_{\mathrm{n}}\dot{u}\ ,\ \tau_1 = K_{\mathrm{s}}v + C_{\mathrm{s}}\dot{v}\ , \tau_2 = K_{\mathrm{s}}w + C_{\mathrm{s}}\dot{w} \tag{4}$$

Where σ and τ are the normal and shear tractions; u , v , and w are the displacement of normal and two shear components; $\dot{u}$, $\dot{v}$, and $\dot{w}$ are the velocity of normal and two shear components; K_{n} and K_{s} are the spring coefficient of normal and shear components; C_{n} and C_{s} are the damping coefficient of normal and shear components; K and C are given as:

$$K_{\mathrm{n}} = \frac{E}{2r}\ ,\ K_{\mathrm{s}} = \frac{G}{2r} \tag{5}$$

$$C_{\mathrm{n}} = \rho c_{\mathrm{p}}\ ,\ C_{\mathrm{s}} = \rho c_{\mathrm{s}} \tag{6}$$

Where r is the distance from wave source to boundary; E is modulus of elasticity; G is shear modulus of elasticity; ρ is density ; c_{p} is pressure wave velocity; c_{s} is shear wave velocity; c_{p} and c_{s} are given as:

$$c_{\mathrm{p}} = \sqrt{\frac{(1-\nu)E}{(1+\nu)(1-2\nu)\rho}}\ ,\ c_{\mathrm{s}} = \sqrt{\frac{E}{2(1+\nu)\rho}} \tag{7}$$

Where ν is Poisson's ratio.

4 The contact nonlinearity of contraction joints

Contraction joints are an important aspect of seismic response of arch dam. During the construction process, the placement of arch dam concrete is divided into several dam sections as a section of 20m width. After concrete cools to the steady temperature and contraction joints grouting between dam sections, dam sections combines into a whole model to resist water load. Under the static load, contraction joints work in compression. During earthquake, the arch tensile stress generated overcomes the arch compressive stress under static load and then contraction joints open. Pacoima arch dam in America has experienced the Richter 6.6 earthquake and dam itself is not damaged, but the opening and closing of contraction joints has obviously occurred. The contact nonlinearity caused by contraction joints attracts the attention of scholars.

Contact problem has clearly physical concept, mainly including opening, closing and slipping of contact surface, and easy to determine the constraint condition. The point is to get appropriate numerical solution method aiming to the discontinuous nonlinear problem.

The contact model can be divided into two categories aiming to the different treatment of constraint condition. One is contact force model based on the nonlinear boundary condition, taking Lagrange multiplier method as representative, and Lagrange multiplier represents the unknown contact force. Another is represented as penalty function. The introduction of contact stiffness into model is to meet the contact boundary constraint condition. To meet the condition of no embedding between contact surface, penalty function method needs to introduce greater stiffness. Theoretically, there still exists embedded distance, and there is a certain sensitivity to the stiffness value. In the contact force model, applying the unknown force as the contact force to the contact interface is to meet the constraint

condition, and there is no problem of artificially assumed stiffness. The Lagrange multiplier method is used in this paper.

The contact surface constraint condition:

a. Opening condition $\begin{cases} (\mathbf{u}_B - \mathbf{u}_A)\mathbf{n} > 0 \quad \lambda_n = 0 \\ \lambda_s = 0 \end{cases}$

b. Closing condition $\begin{cases} (\mathbf{u}_B - \mathbf{u}_A)\mathbf{n} = 0 \quad \lambda_n \geq 0 \\ (\mathbf{u}_B - \mathbf{u}_A)\mathbf{t} = (\mathbf{u}_B^{n-1} - \mathbf{u}_A^{n-1})\mathbf{t}^{n-1} \quad |\lambda_s| < \mu\lambda_n \end{cases}$

c. Slipping condition $\begin{cases} (\mathbf{u}_B - \mathbf{u}_A)\mathbf{n} = 0 \quad \lambda_n \geq 0 \\ (\mathbf{u}_B - \mathbf{u}_A)\mathbf{t} \neq (\mathbf{u}_B^{n-1} - \mathbf{u}_A^{n-1})\mathbf{t}^{n-1} \quad |\lambda_s| = \mu\lambda_n \end{cases}$

Where, the location of point A and B is $\mathbf{u}_A$ and $\mathbf{u}_B$; $\mathbf{n}$ is the direction vector from A to B; λ_s is shear contact force; λ_n is normal contact force; μ is friction coefficient; $\mathbf{t}$, $\mathbf{t}^{n-1}$ is the current step and previous step.

From (3), $\mathbf{A} = \mathbf{M}$, $\mathbf{F} = \mathbf{M}(2\mathbf{U}_n - \mathbf{U}_{n-1}) - \mathbf{K}\mathbf{U}_n dt^2 - \mathbf{C}(\mathbf{U}_n - \mathbf{U}_{n-1})dt + \mathbf{F}_n dt^2$, $\mathbf{U} = \mathbf{U}_{n+1}$, the equation can be written as:

$$\mathbf{A}\mathbf{U} = \mathbf{F} \tag{8}$$

The equation including contact force can be given as:

$$\mathbf{A}\mathbf{U} = \mathbf{F} - \mathbf{B}\boldsymbol{\lambda} \tag{9}$$

Where, $\mathbf{B}$ is contact constraint matrix, $\boldsymbol{\lambda}$ is contact force vector.

Contact constraint equation can be given as:

$$\mathbf{B}^T\mathbf{U} = \boldsymbol{\gamma} \tag{10}$$

Where, $\boldsymbol{\gamma}$ is displacement constraint vector.

From (9) and (10), contact force equation is given as:

$$\mathbf{C}\boldsymbol{\lambda}^l = \mathbf{D}\mathbf{U} \tag{11}$$

Where $\boldsymbol{\lambda}^l$ is contact force vector in the local coordinate system, $\mathbf{C}$ is flexibility matrix , $\mathbf{D}\mathbf{U}$ is displace vector . $\mathbf{C}$ and $\mathbf{D}\mathbf{U}$ are given as:

$$\mathbf{C} = \mathbf{T}\mathbf{B}^T\mathbf{A}^{-1}\mathbf{B}^T\mathbf{T}^T, \quad \mathbf{D}\mathbf{U} = \mathbf{T}\mathbf{B}^T\mathbf{A}^{-1}\mathbf{F} - \boldsymbol{\gamma}^l \tag{12}$$

Where $\boldsymbol{\gamma}^l$ is displace constraint vector in the local coordinate system, $\mathbf{T}$ is coordinate system transformation matrix.

The flexibility matrix of contact force equation $\mathbf{C}$ is full matrix due to added mass considering the effect of dynamic water pressure, normal contact force and shear contact force are coupled each other. The modified Gauss-Seidel iterative method solving normal contact force and shear contact force alternatively is used to solve the equation.

5 Damage model of concrete

Damage and failure of concrete has the following characteristics:
(1) The damage process of these quasi-brittle materials is the initiation and propagation of microcracks.
(2) The tensile strength of concrete and rock is much lower than compressive strength, and its damage is mainly controlled by tensile strength.
(3) Residual deformation can be caused due to not completely closing of crack.
(4) Elastic modulus and strength decrease with the evolution of damage.
(5) During the transformation from tension to compression, due to the closing of crack, elastic modulus returns to the initial value, showing so called 'unilateral effect'.

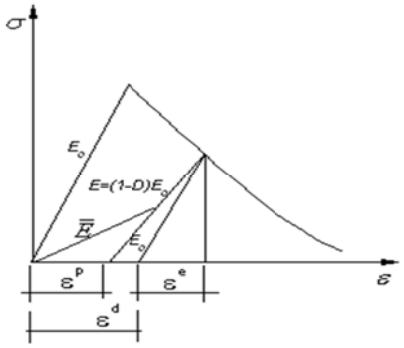

Figure 1 Damage evolution function of concrete under uniaxial cyclic tensile loading

As shown in Figure 1, $\varepsilon = \varepsilon^{e} + \varepsilon^{d}$. Where, ε is total strain; ε^{e} is elastic strain; ε^{d} is damaged strain. Concrete testing results show that under the reciprocating load, if the strain doesn't exceed the initial unloading strain, there is no extra damage and the elastic modulus remain the same. When stress tends to zero, there exists an irreversible strain. Its actual apparent modulus and the corresponding secant modulus changes nonlinearly with stress, and the apparent modulus is less than the corresponding elastic modulus. When the load changes from tension to compression, the elastic modulus recovers the initial value due to the crack closure, showing the so called 'unilateral effect', but need to account for the residue deformation. According to the test results of uniaxial tensile and compressive load, the increasingly irreversible deformation and the damaged elastic modulus under loading and unloading can be got.

The damage model in this paper has borrowed the yield function and the concept of weight factor from multi-axial condition to uniaxial condition from concrete plastic damage model[9].

The yield function is given as:

$$F = \frac{1}{1-\alpha}\left[\alpha I_1 + \sqrt{3J_2} + \beta\langle\hat{\sigma}_1\rangle\right] - c_c = 0 \tag{13}$$

where the I_1 and J_2 are the first invariant of stress and second invariant of stress deviator respectively, and the α and β are the dimensionless constants evaluated by the initial shape of damage surface, which are related to the ratio of equibiaxial to uniaxial compressive strengths and the ratio of compressive to tensile strengths. The constants α and β for concrete are usually taken as 0.12 and 7.68[10].

The weight factor is given as:

$$r(\hat{\boldsymbol{\sigma}}) = \frac{\sum_{i=1}^{3}\langle\hat{\sigma}_i\rangle}{\sum_{i=1}^{3}|\hat{\sigma}_i|} \tag{14}$$

Where, $\langle\sigma\rangle = \frac{1}{2}\left(\sigma + |\sigma|\right)$; If the value of $\langle\ \rangle$ is positive, the value remains same; If the value of $\langle\ \rangle$ is minus, the value changes to zero; $\hat{\sigma}_i$ is effective principle stress.

After concrete is damaged, when the strain under unloading and reloading doesn't exceed the initial unloading strain, its stress is $\sigma = (1-d_t)E_0(\varepsilon-\varepsilon^p)$ and its corresponding apparent elastic modulus is $\bar{E} = (1-d_t)E_0(1-\varepsilon^p/\varepsilon) = (1-d_{tt})E_0$. Where, d_{tt} is the corresponding apparent damage variable. The constitutive equation is $\sigma = \bar{E}\varepsilon$. For multidimensional system, the equivalent damage variable $d = rd_{tt}$ and the constitutive equation is $\boldsymbol{\sigma} = (1-d)\mathbf{D}\boldsymbol{\varepsilon}$. When stress tends to zero, ε_t is close to ε^p. For multidimensional system, ε_{max} is close to ε^p and the strain vector $\boldsymbol{\varepsilon}$ is the corresponding residual strain vector $\boldsymbol{\varepsilon}^p$. When ε_t is less than ε^p, from tension to compression, stiffness recovers the initial value and the constitutive equation is $\sigma = E_0(\varepsilon-\varepsilon^p)$. For multidimensional system, the constitutive equation is $\boldsymbol{\sigma} = (1-d)\mathbf{D}(\boldsymbol{\varepsilon}-\boldsymbol{\varepsilon}^p)$.

6 Parallel computation based on domain decomposition method

The basic idea of domain decomposition method is the use of block, dividing a whole system into several sub-systems. The solution of original system can be changed into the solution of several sub-systems, and the exchange between sub-systems can be achieved by data transferring. Domain decomposition method is divided into steps as follows:

(1) The whole model is divided into several sub-models.
(2) The solution of each sub-model is done in each partition.
(3) The solution of the whole model is got by combining the results of each sub-model.

By overlapping the district or not, domain decomposition method is divided into overlapping domain decomposition method and non-overlapping domain decomposition method. Theoretical foundation of overlapping domain decomposition method is Schwarz alternating method and messaging between sub-models is done through the related district, as shown in Figure 2.

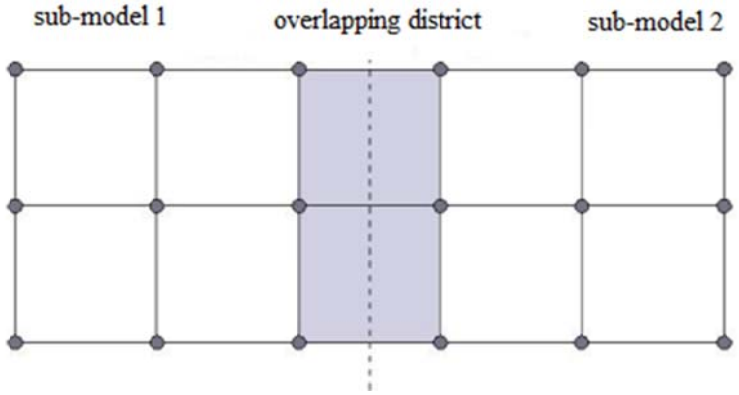

Figure 2 Overlapping district between sub-models

Since the mass matrix is diagonal, the kinetic equation of explicit format is decoupled. Thus, the decoupled equation has the innate advantage of parallel computation. For the computation of each sub-model, at each time step, the displacement, velocity and acceleration on the boundary of each sub-model are updated by exchanging data of the related overlapping district, and then the displacement, velocity and acceleration of the sub-model are got from the new boundary conditions. Thus, the solution of kinematic equation with explicit integral format is done without iteration, simply updating the boundary condition by exchanging data.

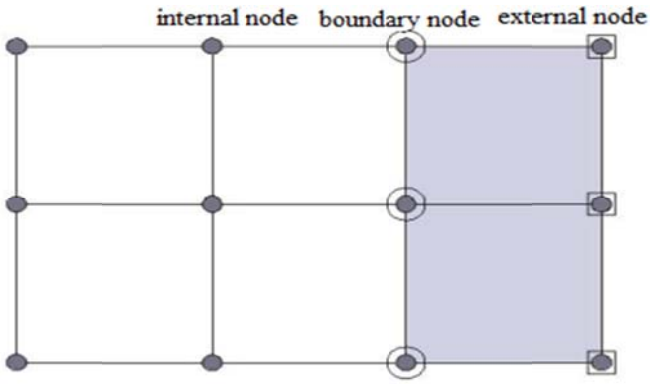

Figure 3 node distribution diagram in each sub-model

As shown in Figure 3, the nodes of each partition are divided into internal nodes, boundary nodes and external nodes, where internal nodes and boundary nodes are solving nodes, and boundary nodes and external nodes are used to exchange information with other sub-models. The boundary nodes of this sub-model is the external nodes of another sub-model, and the external nodes is the boundary of this sub-model. The solution of external nodes is not taken in this sub-model.

Parallel computation structure uses a master-slave programming model, consisting of one master process and several slave processes. Master process is a control program that doesn't participate in the computation and it is responsible for sending data to slave processes and receiving data from slave processes. All messaging occurs between the master process and slave processes. There is no messaging between slave processes and slave processes are only responsible for the corresponding sub-model computation. Messaging is achieved by blocking communication that computation and communication are done sequentially. As shown in Figure 4.

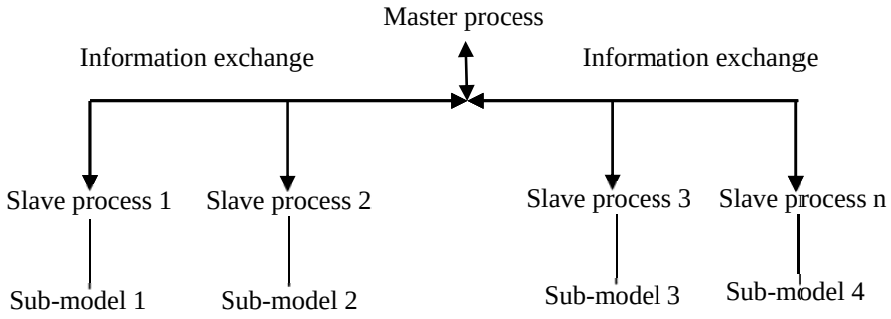

Figure 4 Parallel computation structure

A dam-foundation system with 466381 nodes, 445383 elements and 1399143 degrees of freedom is tested. The whole model is divided into 1-11 sub-models and the parallel computation performance is tested. A multicore computer with 12 CPU is used. The efficiency of parallel computation is shown in Table 1.

Table 1 Parallel computation performance test value

Number of process	Running time(h)	Speedup	Parallel efficiency
1	13.22	1	100%
2	6.93	1.91	96%
4	3.59	3.68	92%
6	2.62	5.05	84%
8	2.11	6.27	78%
10	1.93	6.85	69%
11	1.94	6.81	62%

7 Seismic response of Shapai arch Dam

Shapai dam is a three-center gravity arch structure, of 132m high, completed in 2006, was the world's highest RCC arch dam at the time. On May 12, 2008, Wenchuan in China was attacked by the strong earthquake of M=8.0. The distance from Shapai arch dam to the epicenter is 36 km. Since there was not earthquake recording device at the dam site, the earthquake recording failed to obtain during earthquake. According to the contour map of seismic intensity and bedrock peak acceleration PGA the department announced after the earthquake, the seismic intensity of the Shapai dam site ranges 8 - 9 degrees and PGA ranges between 177gal-286gal. The seismic intensity of the dam site and the corresponding acceleration have exceeded design values. After the earthquake, no damage was found by a thorough inspection of the dam site. Since no ground motion has been recorded at the dam site during the earthquake, it has to be reestablished by using the "stochastic finite fault method" and parameters identified by the accelerograms recorded at 7 stations during the earthquake. Fig. 13 is the reestablished 3 components of the artificial accelerograms for the Shapai dam site with PGA of 0.262 g and long duration of more than 40 minutes. The seismic wave is shown as Figure 5.

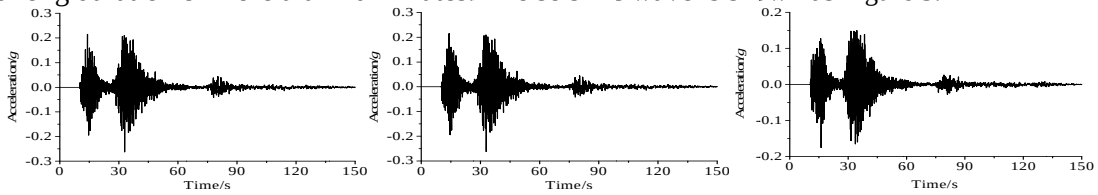

Figure 5 reestablished artificial accelerograms at Shapai dam site (from Zhang Cuiran)

Finite element model: As shown in Figure 6, the total number of nodes, elements, and degrees of freedome are 425568 , 404090, and 1276704, respectively. The dam and near field is modeled by nonlinear material model, so through the height direction of dam, the grid length of dam is taken as 2m. Through the thickness direction of dam, the dam is divided into 11 parts. According the cross river direction, the grid length of dam is taken as 2m. The grid length of near foundation is about 3m. As shown in Figure 7, the total number of nonlinear material elements is182867, which is 45% of the total number of elements. The number of dam nodes and elements is 67326 and 58757 respectively, including 2112 contact point pairs modelling contracting joints and induced joints. The element size of elastic foundation rock mass is about 10-25 m.

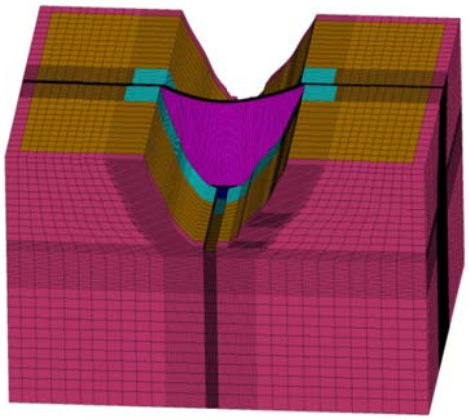

Figure 6 FEM mesh of dam-foundation system

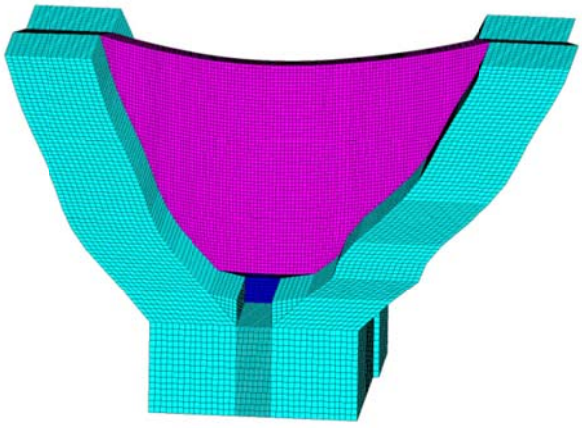

Figure 7 FEM mesh of nonlinear elements

The concrete material parameters are taken as: density $\rho = 2400\,\mathrm{kg/m^3}$, original elastic modulus $E_0 = 18\,\mathrm{GPa}$, Poisson ratio $\mu = 0.167$, dynamic tensile strength $f_{t0} = 4.3\,\mathrm{MPa}$, fracture energy $G_F = 296\,\mathrm{N/m}$, Figure 8 and Figure 9 show the adjusted function of cracking displacement to the degradation tensile strength $w - f_t$ and to the damage variable $w - D$.

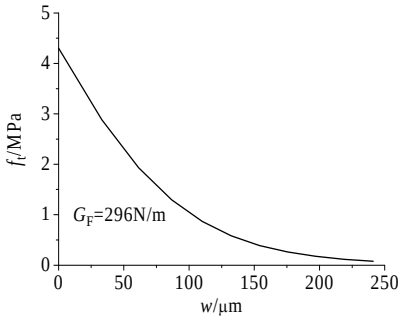

Figure 8 $w-f_t$

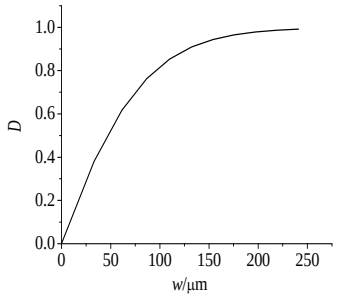

Figure 9 $w-D$

The rock material parameters are taken as: density $\rho=2600\,\mathrm{kg/m^3}$, original elastic modulus $E_0=11\mathrm{GPa}$, Poisson ratio $\mu=0.23$, friction angel $\varphi=47.73^\circ$, cohesive stress $c=2.0\,\mathrm{MPa}$, dynamic tensile strength $f_{t0}=2c\cdot\cos\varphi/(1+\sin\varphi)=1.55\,\mathrm{MPa}$, $G_F=107\,\mathrm{N/m}$. The parameters of viscous damping boundaries of the foundation are taken as: $K_n=1.61\cdot10^7\,\mathrm{N/m^3}$, $C_n=5.76\cdot10^6\,\mathrm{N\cdot s/m^3}$, $K_s=0.65\cdot10^7\,\mathrm{N/m^3}$, $C_n=3.41\cdot10^6\,\mathrm{N\cdot s/m^3}$. Figure 10 and Figure 11 show the adjusted function of cracking displacement to the degradation tensile strength $w-f_t$ and to the damage variable $w-D$.

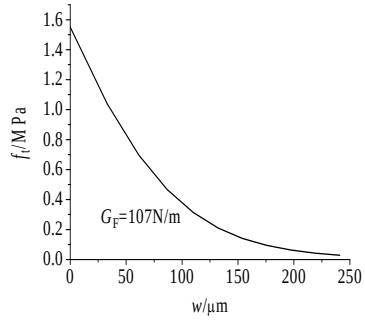

Figure 10 $w-f_t$

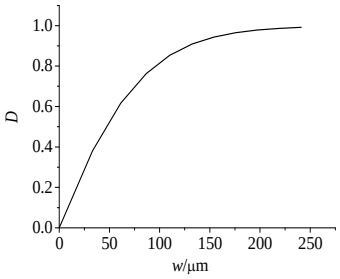

Figure 11 $w-D$

The shear strengths of contraction and induced joints are taken as: f=1.1, c=1.1MPa. The tensile strength of contraction joints and induced joints are zero and half of the tensile strength of concrete, respectively.

Damage model for concrete and rock:

Figure 12 shows that the dam is basically not damaged even near the bottom pedestal, but the jointed foundation rock body is damaged, as the tensile strength and fracture energy of the cracked foundation rock body are less than those of the dam concrete.

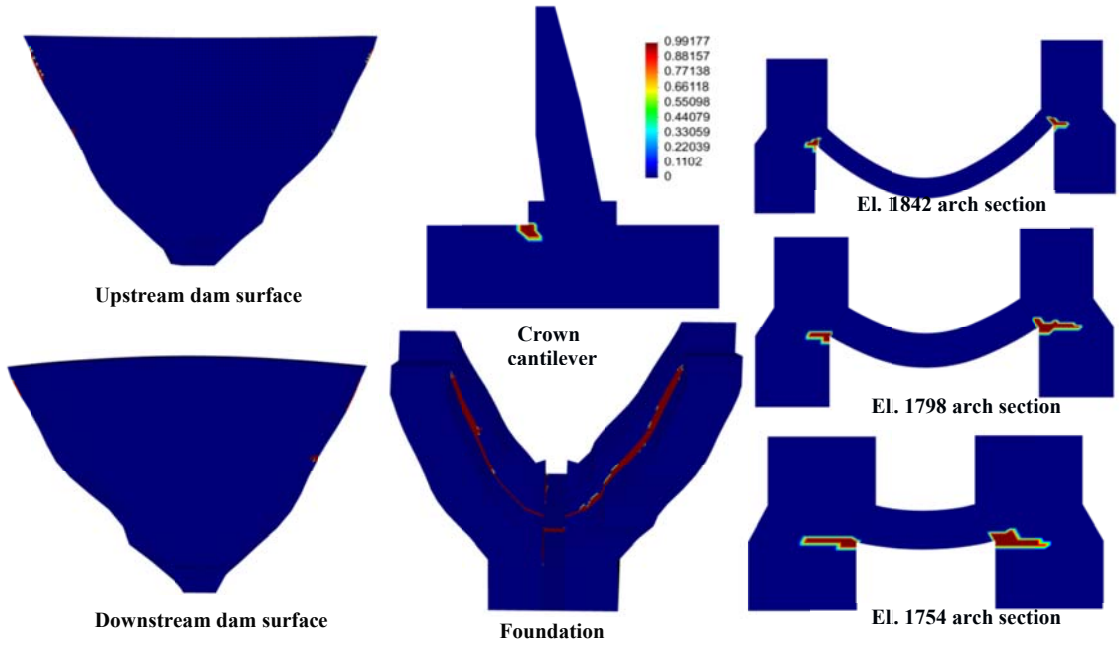

Figure 12 Damage of jointed foundation rock masses

Damage model for concrete and Drucker-Prager elastoplastic model for rock: Figure 13 shows that dam is damaged near the bottom pedestal and the jointed foundation rock is damaged in the plastic form.

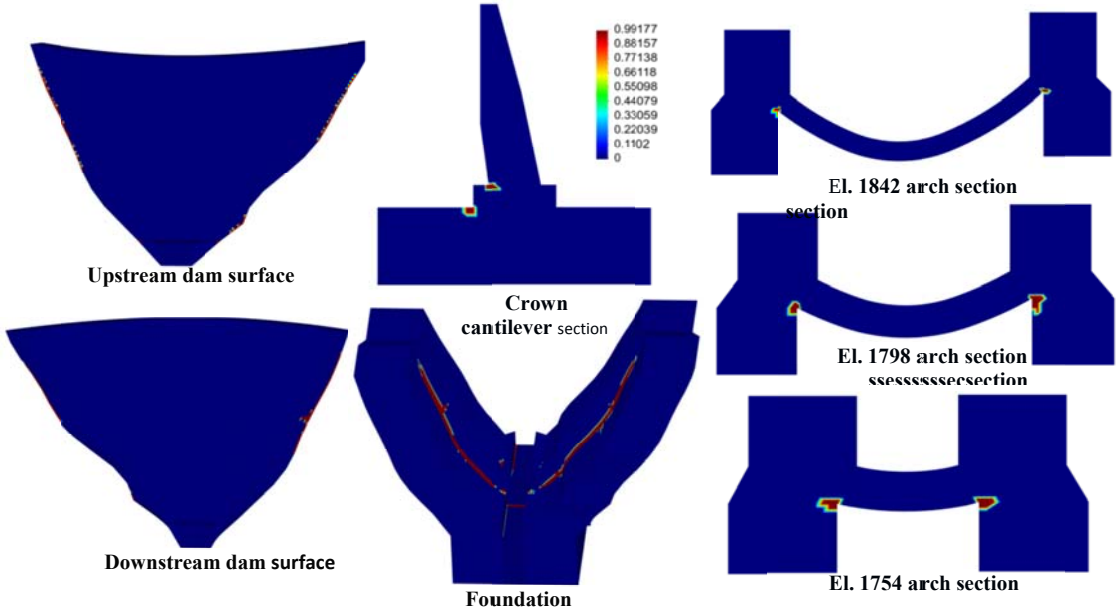

Figure 13 Damageable model for dam with Druker-Prager model for foundation rock masses

Damage model for concrete and elastic model for rock: Figure 14 shows that the dam is significantly damaged due to stress concentration near the interface with foundation and, especially, near the bottom pedestal.

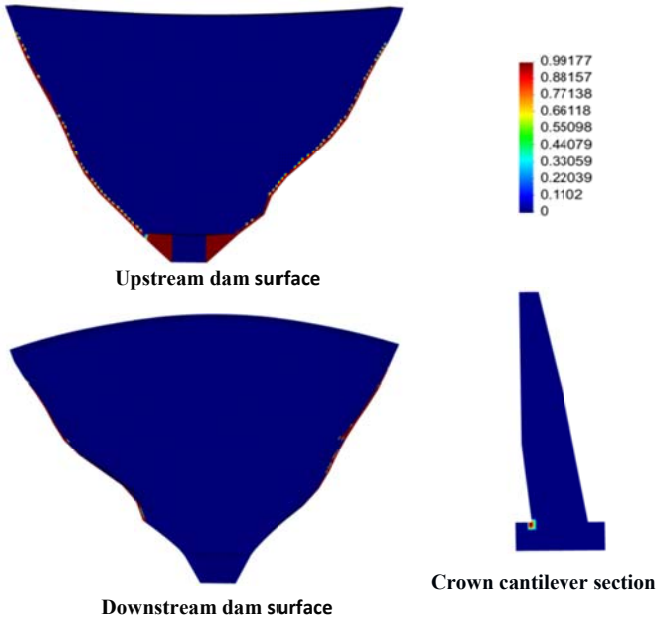

Figure 14 Damageable dam with elastic foundation

By comparing all the models, it seems that the results of both considering damage model of concrete and rock. is more appropriate for verifying the behavior of the Shapai arch dam during the Wenchuan Earthquake.

Conclusions

In this study, a relatively complete nonlinear dynamic analysis model of arch dam-foundation system based on finite element method in the time domain is presented. The seismic damage process of Shapai dam-foundation system is investigated by using damage model applied to dam-foundation system. As comparative studies, the seismic damage process of dam-foundation system is investigated by using damage model for dam, using Drucker-Prager elastoplastic and elastic model for rock mass. Based on the present numerical analysis, some conclusions are drawn:

1 The damage evolution both of the dam and foundation rock masses should be considered. The usually jointed foundation rock masses with micro fissures will be damaged earlier than the dam during strong earthquake.

2 Using the Druker-Prager and elastic model for evaluating the damage of the foundation rock masses may not reflect the reality.

3 Given the complexity of dynamic property of rock material and the difficulty of experimental verification, there is not a widely recognized rock damage model and further investigation is needed.

REFERENCES

1 Cervera M, Oliver J, and Faria R(1995), seismic evaluation of concrete dams via continuum damage models, Earthq.Eng. Struc. Dyn., 24 1225-1245.

2 Zhong H, Lin G, Li X and Li J (2011), Seismic failure modeling of concrete dams considering heterogeneity of concrete, Soil Dyn. Earthq. Eng. 31(12) 1678-1689.

3 Pan J, Zhang C, Xu Y and Jin F(2011), A comparative study of the different procedures for seismic cracking analysis of concrete dams, Soil Dyn. Earthq. Eng. 31(11) 1594-1606.

4 Hariri-Ardebili M A and Mirzabozorg H(2013), A comparative study of seismic stability of coupled arch dam-foundation-reservoir system using infinite element and viscous boundary models, Int. J. Struct. Stab. Dy. 13(6) 1350032 (24 pages).

5 Chopra A K, et al(1922). Modeling of dam-foundations interaction in analysis of arch dams . Proc. 10th WCEE. Madrid, 8.

6 Dominguez J, et al(1992). Model of the seismic analysis of arch dams including interaction effects . Proc. 10th WCEE. Madrid, 8.

7 Tu J(1999), Nonlinear seismic response analysis of high concrete dam–foundation system with cracked surface, Ph.D. Thesis, China Institute of Water Resources and Hydropower Research.

8 Liu J B, Lu Y D(1998), A direct method for analysis of dynamic soil-structure interaction. China Civil Engineering Journal, 31(3):55-64.

9 J. Lee and G. L. Fenves(1998), Plastic-damage model for cyclic loading of concrete structures, *J. ENG. MECH-ASCE.* 124(8) 892-900.

10 J. Lubliner, J. Oliver, S. Oller and E. Onate(1989), A plastic-damage model for concrete, *Int. J. Solids. Struct.* 25(3) 299-326.